Laser and Particle Beams (2009), *27*, 699–707.

doi:10.1017/S0263034609990425

Nickel-based super-alloy Inconel 600 morphological modifications by high repetition rate femtosecond Ti:sapphire laser

J. STASIC,[1] B. GAKOVIC,[1] A. KRMPOT,[2] V. PAVLOVIC,[3] M. TRTICA,[1] AND B. JELENKOVIC[2]

[1]VINCA Institute of Nuclear Sciences, Belgrade, Serbia
[2]Institute of Physics, Belgrade, Serbia
[3]FOA, Department of Mathematics and Physics, Belgrade, Serbia

(RECEIVED 19 June 2006; ACCEPTED 8 September 2009)

Abstract

The interaction of Ti:sapphire laser, operating at high repetition rate of 75 MHz, with nickel-based super-alloy Inconel 600 was studied. The laser was emitting at 800 nm and ultrashort pulse duration was 160 fs. Nickel-based super-alloy surface modification was studied in a low laser energy/fluence regime of maximum 20 nJ–15 mJ/cm^2, for short (10 s) and long irradiation times (range of minutes). Surface damage threshold of this material was estimated to be 1.46 nJ, i.e., 0.001 J/cm^2 in air. The radiation absorbed from Ti:sapphire laser beam under these conditions generates at the surface a series of effects, such as direct material vaporization, plasma creation, formation of nano-structures and their larger aggregates, damage accumulation, etc. Laser induced surface morphological changes observed on Inconel 600 were: (1) intensive removal of surface material with crater like features; (2) material deposition at near and farther periphery and creation of nano-aggregates/nano-structures; (3) sporadic micro-cracking of the inner and outer damage area. Generally, features created on nickel-based super-alloy surface by high repetition rate femtosecond pulses are characterized by low inner/outer damage diameter of less than 11 μm/30 μm and relatively large depth on the order of 150 μm, in both low (10 s) and high (minutes) irradiation time regimes.

Keywords: Femtosecond; Laser-matter interaction; Nickel-based super-alloy Inconel 600; Ti:sapphire laser

1. INTRODUCTION

Studies of the surface modification of materials, including metals and alloys, by various types of energetic beams (laser beams among others), are of great fundamental and technological interest. Laser surface modification studies are almost as old as the laser itself. Due to dramatic decrease of thermal effects, high precision processing of the materials using ultrashort laser pulses (both picosecond and femtosecond) is extremely advantageous (Semaltianos *et al.*, 2002; Gamaly *et al.*, 2005). Picosecond as well as femtosecond lasers are widely applied for the surface modification of metals (Gamaly *et al.*, 2005; Di Bernardo *et al.*, 2003; Bussoli *et al.*, 2007), alloys (Trtica *et al.*, 2009), biomaterials (Mirdan *et al.*, 2009), etc. The studies of ion and X-ray emission from plasma, induced by ultrashort laser, in front of metallic targets are also highly important (Chaurasia *et al.*, 2008).

Surface modification studies of nickel-based super-alloys by various types of laser beam are also highly significant. The last decade saw some of the studies of laser beam interaction with these alloys. Beams of the pulsed Nd:YAG (Chen *et al.*, 1996; Bugayev *et al.*, 2006), excimer (Pantelis & Psyllaki, 1996), pulsed/cw CO_2 (Zysk, 1990; Hong *et al.*, 2008), and Ti:sapphire laser (Feng *et al.*, 2005; Semaltianos *et al.*, 2009) have so far been employed for these studies.

Studies of the interaction of pulsed femtosecond Ti:sapphire laser beam with nickel-based super-alloys are not extensively reported in the literature. These materials are within a class of special alloys characterized by extraordinary properties: high temperature and mechanical strength, admirable corrosion resistance, excellent thermal conductivity, resistance to aggressive atmosphere. They are therefore attractive for various applications in electronic, chemical and food industry, aero-space engineering, etc. Moreover, these

Address correspondence and reprint requests to: Biljana Gaković, Atomic Physics Laboratory, VINCA Institute of Nuclear Sciences, P.O. BOX 522, 11001 Belgrade, Serbia. E-mail: biljagak@vinca.rs

super-alloys can be used in nuclear complexes, in fission as well as fusion reactor technology (In *et al.*, 1995; Busharov *et al.*, 1977).

The interaction of the nickel-based super-alloy Inconel 600 with femtosecond pulses at a megahertz repetition rate has not been described in the literature as far as we know. Our emphasis here is on studying the effects of a high repetition rate (75 MHz) femtosecond laser, emitting radiation at 800 nm, on the Inconel 600 surface. Irradiation was performed at low energy—nano-joule regime. Special attention was paid to morphological surface modification of the Inconel as well as to the creation of nano-structures.

2. EXPERIMENTAL

Our experimental setup is shown in Figure 1. The laser used in the experiment was femtosecond Ti:sapphire laser (MIRA 900, Coherent Inc, Santa Clara, CA.). When pumped by a 10 W laser light at 532 nm (VERDI V-10, Coherent Inc.), the average power of the femtosecond laser, at 800 nm, was 2 W. The pulse length and the repetition rate of the laser were 160 fs and 75 MHz, respectively. During the irradiation process, the laser was operated in the fundamental transverse mode. The laser beam was linearly polarized. Irradiation was carried out in air, at atmospheric pressure, and standard humidity. A small part (around 1%) of the femtosecond laser light was split from the main part of the laser beam using a beam-splitter cube and directed to the fast photo-diode for real time monitoring of the femtosecond regime. The signal from the fast photo-diode was monitored by the oscilloscope. The femtosecond laser beam was first expanded, using a beam expander, and then focused using the triplet lens system, with a focal length of 15 mm (FTL, Casix, Fujian, China), mounted on a high precision table with the resolution of 10 μm. The laser beam waist at the lens focus was about 25 μm. The sample was placed at the high precision holder, operating in *x*- and *y*-directions, perpendicular to the laser beam axis. The average power during the experiment was monitored by an Ophir pyroelectric sensor (Lake Oswego, Oregon). Its maximum value at the sample surface was 1.5 W, corresponding to the maximum energy of 20 nJ per pulse.

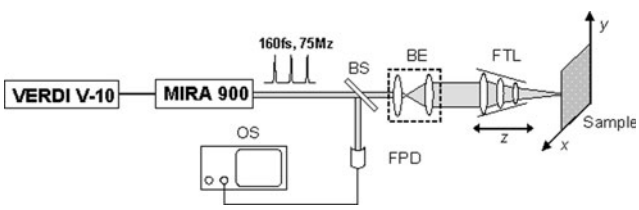

Fig. 1. Experimental setup for irradiation of Inconel 600 superalloy by femtosecond laser. VERDI V-10 and MIRA 900 are pumping solid-state Nd:YVO4 laser, and femtosecond Ti:sapphire laser, respectively. BS, beam splitter; BE, beam expander; FTL, focusing triplet lens (commercial production); FPD and OS, are fast photo-diode and oscilloscope, respectively.

Prior to laser irradiation, the surface of the nickel-based super-alloy Inconel 600 was prepared by a standard metallographic procedure. This included polishing, rinsing, and drying. Bulk dimensions of the samples were 16 mm × 13 mm × 3 mm. Surface roughness was around 120 nm.

Various analytical techniques were used to characterize the Inconel 600 before and after laser irradiation. Crystal phases were identified by X-ray diffractometry. Surface morphology was monitored by optical and scanning electron microscopy. Scanning electron microscopy was connected to an energy dispersive analyzer (EDX) for determining surface composition of the targets. Also, for additional verification of the target elemental composition, the Inductively Coupled Plasma method was applied. Profilometry (Taylor-Hobson Ltd., Leicester, UK) was used to specify the geometry of the ablated/damaged area.

3. RESULTS AND DISCUSSION

The phase composition and the crystalline structure of the Inconel 600 were determined by X-ray diffraction. Angles 2θ in the range from 30° to 100° were scanned by a step of 0.02° in time sequences of 0.5 s. X-ray diffractometry analysis of nickel-based super-alloy, prior to laser irradiation, confirmed its crystalline structure. The sample exhibited a face centered cubic nickel structure with the lattice parameter $a = 3.5806(7)$ Å. The main alloying elements are incorporated in the basic lattice.

Inductively coupled plasma elemental analysis of a non-irradiated sample showed that the target contained mainly nickel (76 wt%), Cr (15.5 wt%), and Fe (8.0 wt%), balanced to 100% by other elements. The target composition measured by EDX method coincided well with the inductively coupled plasma results.

Investigation of the morphological changes induced by femtosecond laser on nickel-based super-alloy (Inconel 600) has shown their dependence on laser beam characteristics, primarily on the laser energy, laser peak power, irradiation time (exposure)/number of accumulated pulses. Morphological changes of Inconel 600 for irradiation times of 10 s and 1, 2, 3, 5, 6, and 7 min are presented in Figures 2, 3, and 4, 6–8, respectively. The irradiation was performed at low laser energy/fluence regime. The laser radiation energy (LRE) during experiments was maximum 20 nJ, and fluence less than 15 mJ/cm^2. These LRE induced significant surface modifications of the Inconel 600 surface. The results of the induced modifications at different irradiation time are presented below.

3.1. Short Irradiation Time (Range of Seconds)

After an irradiation time of 10 s at LRE of 16 and 17.3 (Fig. 2) and 20 nJ (Fig. 3), the damage of the Inconel 600 is clearly visible. Surface changes/phenomena can be summarized as follows: (1) intensive removal of surface material with crater like characteristics (Fig. 2); (2) appearance of

https://doi.org/10.1017/S0263034609990425 Published online by Cambridge University Press

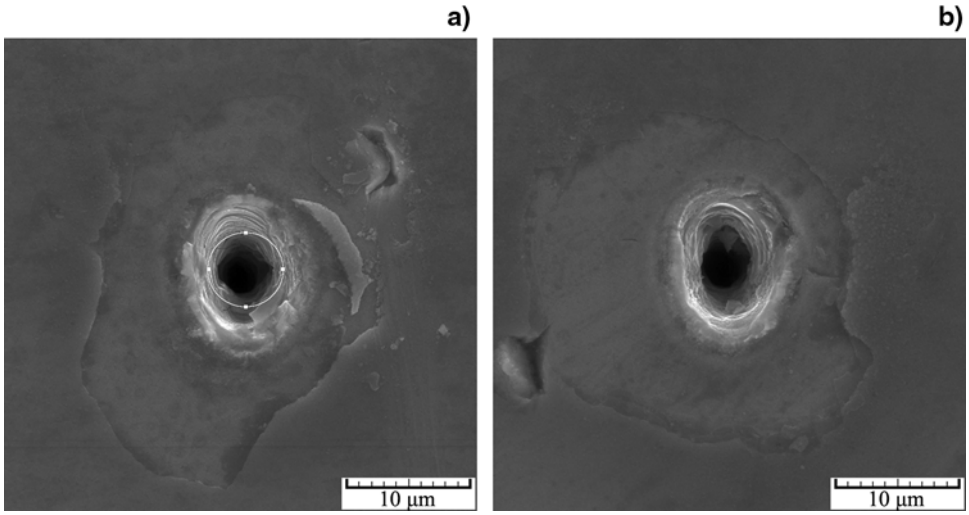

Fig. 2. SEM micrographs of laser radiation effect on super-alloy Inconel 600, at the laser pulse energy of (**a**) 16 and (**b**) 17.3 nJ. Laser pulse length was 160 fs, irradiation time 10 seconds, and pulse repetition rate 75 MHz.

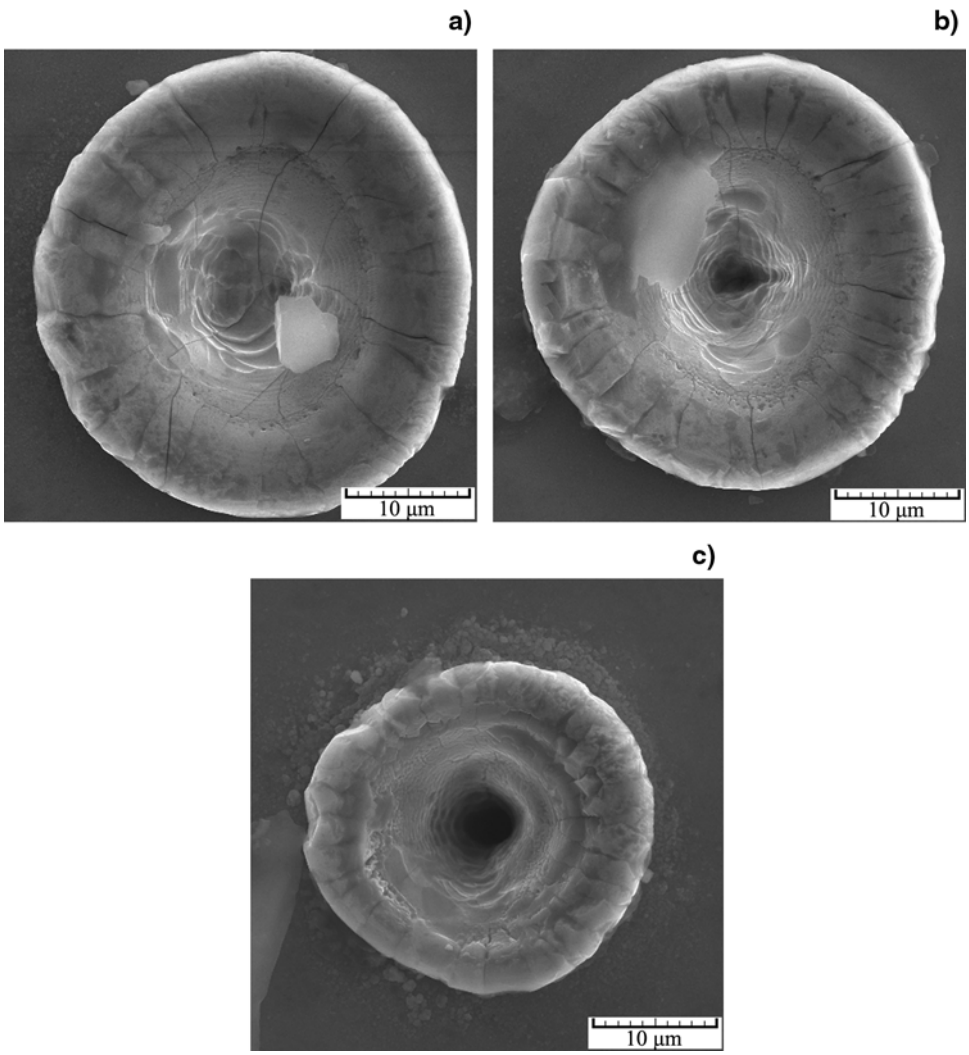

Fig. 3. The effect of 20 nJ, 160 fs laser pulse on super-alloy Inconel 600, at (**a**) 120 and (**b**) 90 μm in front, and (**c**) 20 μm beyond the focus (laser irradiation time 10 s, pulse repetition rate 75 MHz, SEM analysis).

https://doi.org/10.1017/S0263034609990425 Published online by Cambridge University Press

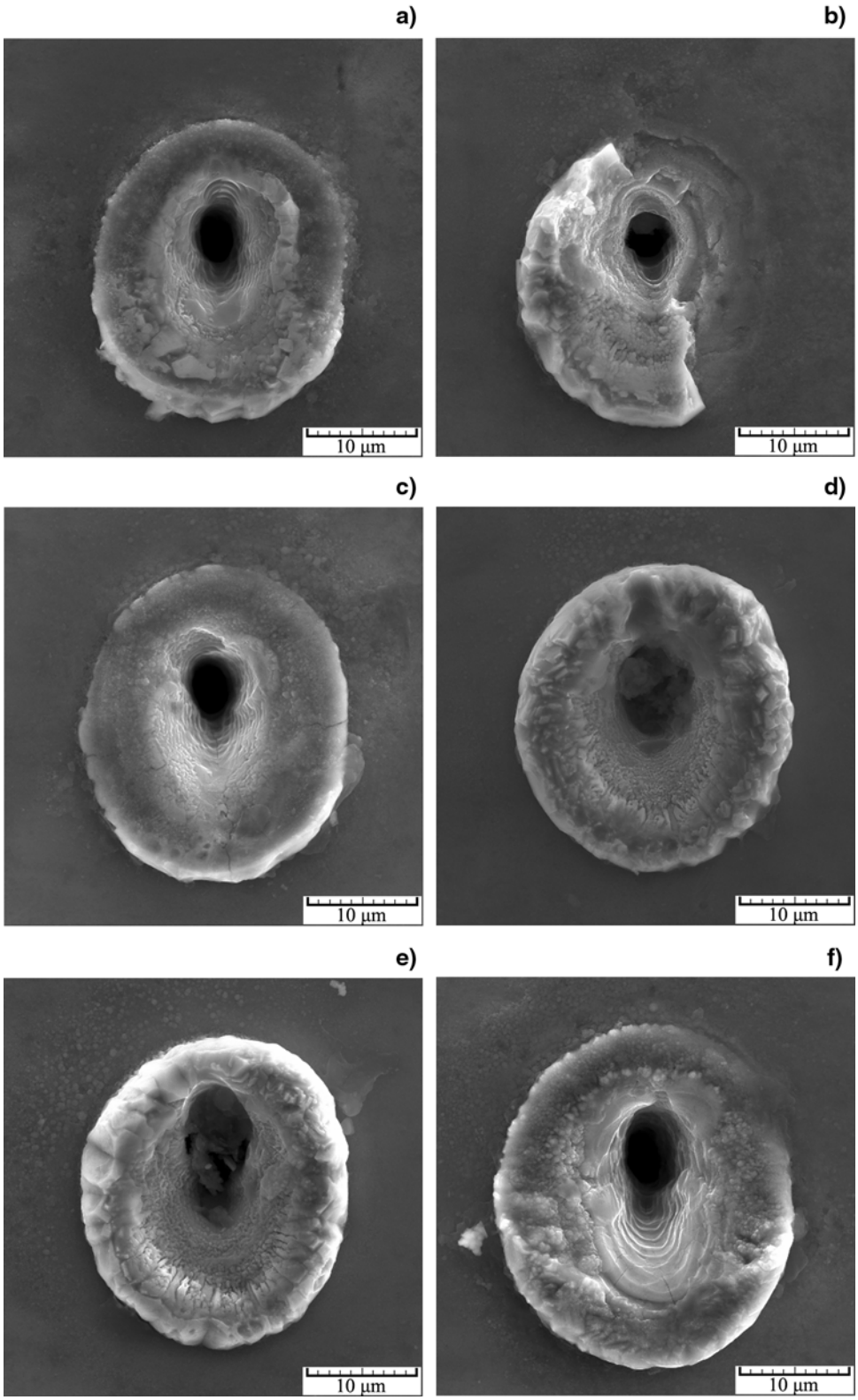

Fig. 4. The effect of 20 nJ, 160 fs laser pulse on super-alloy Inconel 600, as a function of irradiation time: (**a**) 1, (**b**) 2, (**c**) 3, (**d**) 5, (**e**) 6, and (**f**) 7 min (pulse repetition rate 75 MHz, SEM analysis).

redeposited material at near and farther periphery, especially at 20 nJ (Fig. 3); (3) sporadic micro-cracking of the inner and outer damage area; (4) occurrence of relatively sharp rim at lower LRE (16 and 17.3 nJ, Fig. 2) and, (5) spark-like plasma in front of the target. Interaction of Ti:sapphire laser with Inconel 600, under these conditions, resulted in

https://doi.org/10.1017/S0263034609990425 Published online by Cambridge University Press

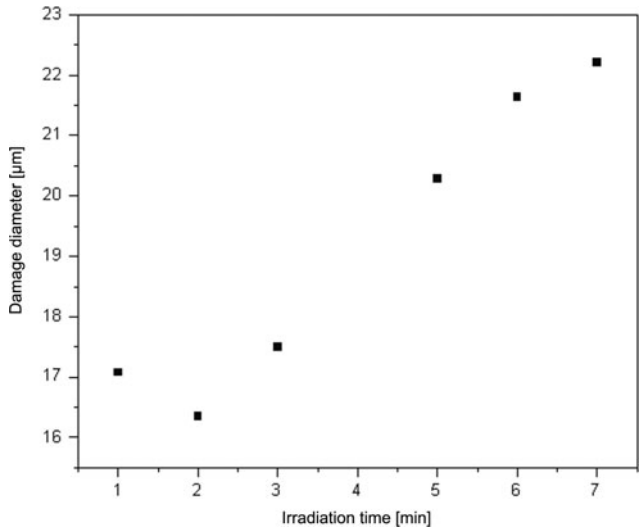

Fig. 5. Damage diameter as a function of laser irradiation time at the constant pulse energy of 20 nJ.

the production of narrow damage area with the presence of debris at the periphery. The equivalent crater diameter of the damage zone was maximum 7 μm (Fig. 2A), while the debris cohesion with the target is low. Large parts of debris produced after irradiation can easily be mechanically removed from the surface (Fig. 2B). On the other hand, material ablation with longer laser pulses, as a rule, results in a harder removal of debris at the periphery even under conditions of aggressive action (Tan *et al.*, 2009). A profilometer analysis of the sample after irradiation with LRE of 20 nJ (Fig. 3A) showed that the crater depth was approximately 4 μm.

3.2. Long Irradiation Time (Range of minutes)

After exposure time of 1, 2, 3, 5, 6, and 7 min at LRE of 20 nJ (Fig. 4), the Inconel 600 surface was modified. Surface features/phenomena can be summarized as follows: (1) intensive removal of surface material with deep crater formation; (2) deposition of the material at near and farther periphery, and occurrence of clusters with nano-structure units; (3) sporadic micro-cracking effects, especially at the rim area; and (4) appearance of plasma in front of the target. Generally, longer irradiation time on the order of minutes resulted in a prominent debris presence at the periphery region and deeper craters as compared to seconds time range (Fig. 4). The maximum crater depth was around 150 μm (Fig. 4F). Cohesion of the material surrounding craters with the target is again low, thus it can be partially removed from the surface (Fig. 4B). Damage diameter as a function of irradiation time, at the constant laser energy, typically increases with the increase of exposure time (Fig. 5).

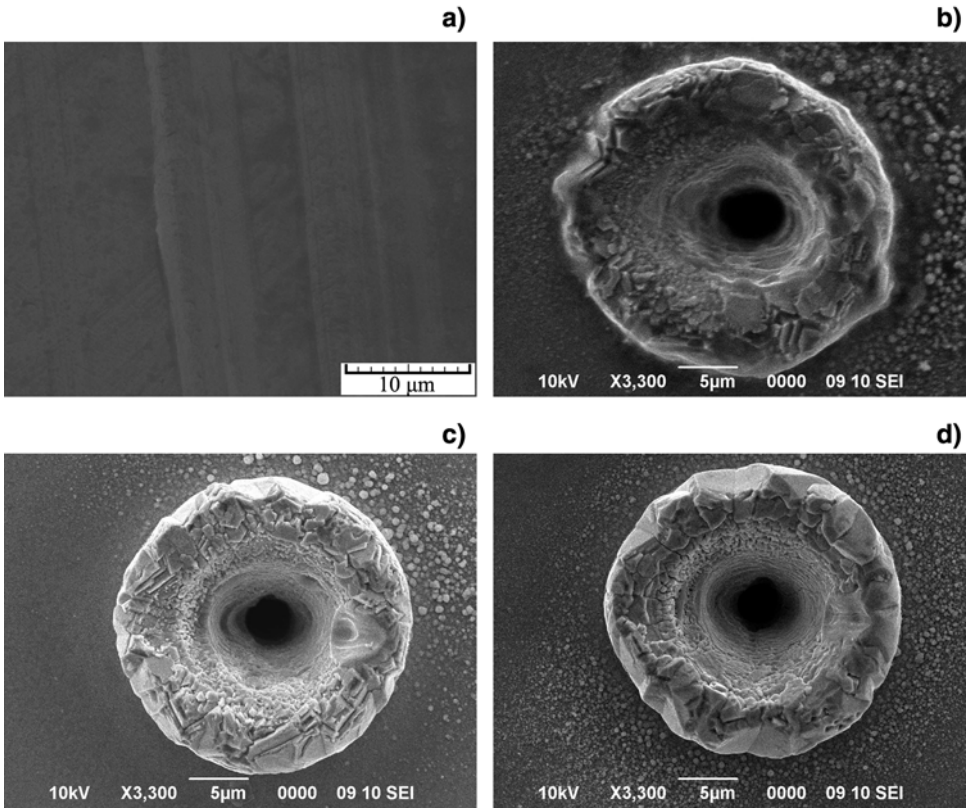

Fig. 6. Morphology effects on super-alloy Inconel 600 for different laser pulse energies at the constant irradiation time of 7 min: (**b**) 20, (**c**) 17.3, and (**d**) 14.7 nJ (pulse repetition rate 75 MHz, SEM analysis). Micrograph (**a**) represents a non-irradiated alloy surface.

https://doi.org/10.1017/S0263034609990425 Published online by Cambridge University Press

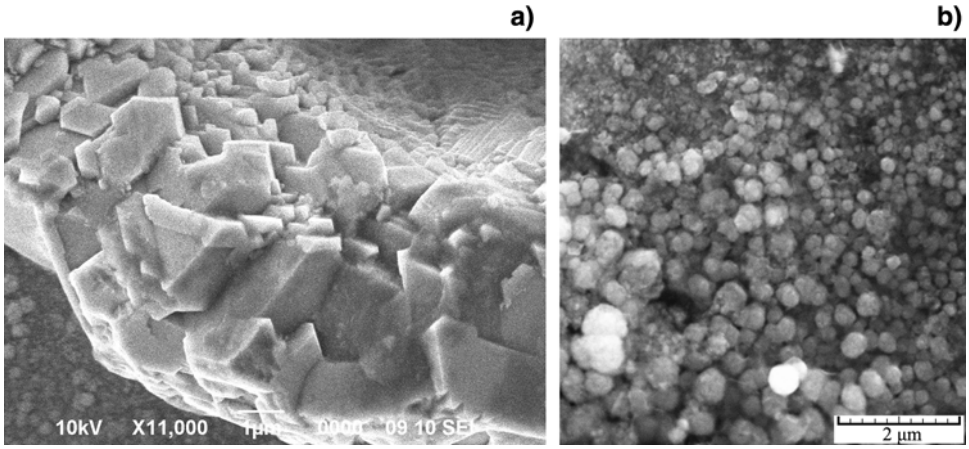

Fig. 7. The view of a crater rim (**a**) and periphery (**b**) of irradiated surface on the super-alloy Inconel 600 (160 fs laser pulse, laser energy 19 nJ, irradiation time 7 min, pulse repetition rate 75 MHz, SEM analysis).

Minimum diameter of about 16 μm was registered after 2 min exposition. From these results we have estimated the ablation threshold of the Inconel 600 alloy. The ablation threshold is defined as the minimum laser radiation energy/fluence required for creating detectable damage on the material. In our experiment of femtosecond Ti:sapphire-Inconel 600 interaction, it was calculated to be around 1.46 nJ, i.e., 0.001 J/cm^2 (Ti:sapphire laser: $\tau = 160$ fs; $\lambda = 800$ nm; repetition rate = 75 MHz). These values were estimated based on the results presented in Figure 6 using method given by Liu (1982) and Semaltianos *et al.* (2009). In this calculation, the laser ablated square diameter D^2 is given by the relation,

$$D^2 = 2\omega_0^2 \ln\left(\frac{F_0^{pk}}{F_{th}}\right) = 2\omega_0^2 \ln\left(\frac{E_p}{E_{th}}\right), \quad (1)$$

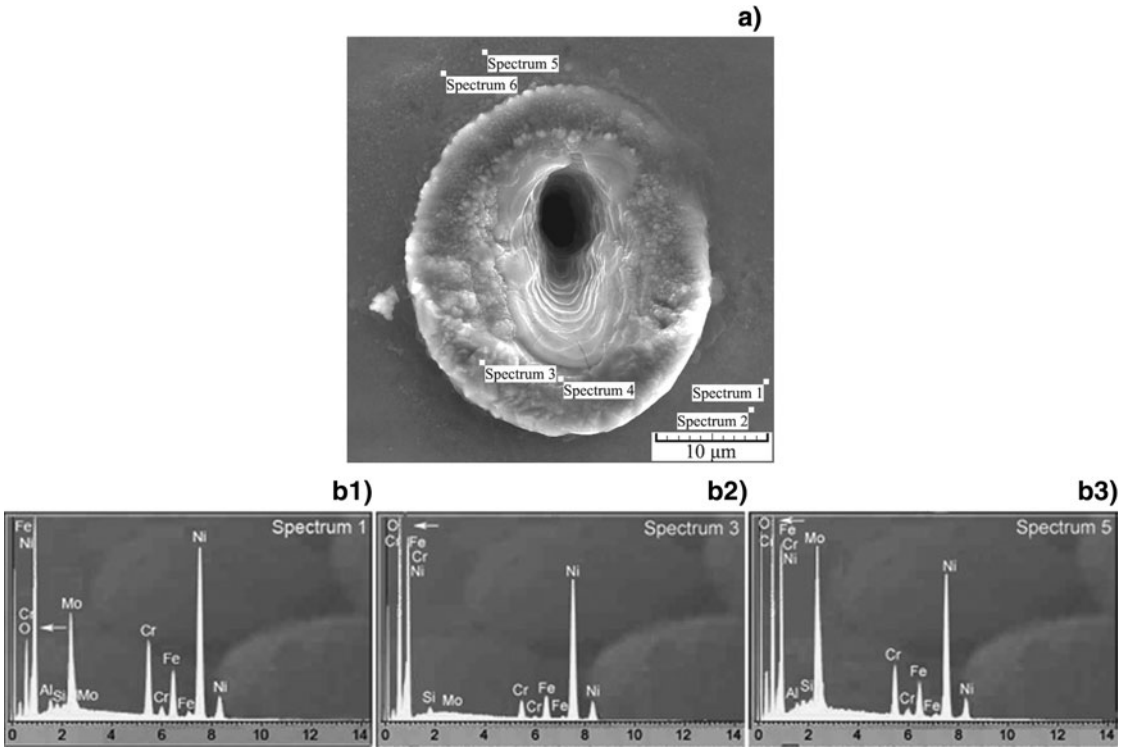

Fig. 8. Locations for EDX analysis on super-alloy Inconel 600 (**a**). Spectra 1 and 2 correspond to a non-irradiated area (**b1**), spectra 3 and 4 to the crater rim (**b2**), and spectra 5 and 6 were taken from the nano-structure zone (**b3**). Laser energy was 20 nJ and irradiation time 7 min.

https://doi.org/10.1017/S0263034609990425 Published online by Cambridge University Press

where F_0^{pk}, ω_0, and E_p represent the fluence, the laser beam radius, and the laser pulse energy (related to F_0^{pk}), respectively. F_{th} and E_{th} are threshold fluence and threshold pulse energy, respectively. The laser beam radius at $1/e^2$ of the laser maximum intensity was used, while F_0^{pk} is given by the relation,

$$F_0^{pk} = \frac{2E_p}{\pi\omega_0^2}. \quad (2)$$

The calculated beam radius ω_0 was about 12 μm. The other available studies concerning the ablation threshold of nickel-based super-alloys irradiated by femtosecond Ti:sapphire laser are mostly dealing with lower frequencies, higher fluences and different types of nickel-based super-alloys. The single pulse ablation threshold for a femtosecond Ti:sapphire-nickel-based super-alloy interaction in air was reported (Semaltianos *et al.*, 2009; Feng *et al.*, 2005; Ma *et al.*, 2007). In these references, the nickel content in super-alloy, as well as the repetition rate (RR) used, were lower than in our case. The single pulse ablation threshold of 0.26 J/cm^2 was reported for C263 super-alloy; Ti:sapphire laser: $\tau =$ 180 fs; $\lambda = 775$ nm; RR = 1 kHz (Semaltianos *et al.*, 2009), 0.33 J/cm^2 for MK-4 super-alloy; Ti:sapphire laser: $\tau = 150$ fs; $\lambda = 780$ nm; RR = 1 kHz (Feng *et al.*, 2005), and 0.3 J/cm^2 in case of CMSX super-alloy; Ti:sapphire laser: $\tau = 150$ fs; $\lambda = 780$ nm; RR = 125 Hz (Ma *et al.*, 2007). Semaltianos *et al.* (2009) showed that the ablation threshold significantly decreases in case of multiple pulse accumulation, and after 100 pulses it is 0.06 J/cm^2.

When ultrashort laser pulse acts on a metal target, a diversity of physical processes is triggered. Generally, depending on the laser energy/fluence used in femtosecond laser irradiation, the material modification/ablation mechanisms can be: (1) normal vaporization; (2) phase explosion; (3) spoliation, and; (4) fragmentation (Bäuerle, 2003; Oh *et al.*, 2007). Irradiation of the nickel-based supper-alloy (Inconel 600) in the regime of low laser energy, resulted probably in a direct solid-vapor (or solid-plasma) transition, including possible phase explosion phenomenon (Cheng & Xu, 2005).

Ablation/modification with femtosecond (ultrashort) laser pulses involves achieving of relatively high intensity (in our experiments), the reduction of the laser penetration depth (LPD) and precise material modification. LPD, for laser-target interaction near threshold, is proportional to α^{-1} (α is the optical absorption coefficient), and in our case (the alloy rich with nickel) it is about 40 nm (Bonse *et al.*, 2000; Semaltianos *et al.*, 2009).

Relatively high laser intensity on the order of about 10^{11} W/cm^2 used in our experiment was enough to stimulate/initiate plasma in front of the target. In contrast to the growth of a metal-vapor plume, which develops on the time-scale of tens to hundreds of picoseconds after the ablation, recent investigation showed that the early-stage plasma creates during the first several picoseconds. This confirms that the plasma in front of the target can not affect the laser radiation absorption/propagation for femtosecond-laser, since the pulse is terminated long before plasma creation.

All irradiations in this work were accompanied by changes in the appearance/shape of rim structure, as well as by the occurrence of sub-micro-/nano-structures (at farther periphery).

For repetition rates higher than 1 MHz, and low pulse energy, only small portion of Gaussian beam close to the intensity peak has enough energy to ablate the material, thus resulting in crater diameter smaller than the laser beam waist. However, at the outer edges of the beam, thermal effect accounts for part of the ablation process even at femtosecond pulse duration. Therefore, thermal defects are drastically reduced but not completely eliminated (Eaton *et al.*, 2005; Osellame *et al.*, 2005; Lam *et al.*, 2007; Ancona *et al.*, 2008; Tan *et al.*, 2009).

The presence of nano-structures at a farther periphery was recorded (Figs. 3, 4, 6, 7), particularly for longer laser irradiation times (order of minutes). It can be concluded from the scanning electron microscope analysis that nano-units are grouped in larger aggregates. Typical dimensions of the individual nano-grain were in the interval from about 50 to about 200 nm (Fig. 7B). After absorption of laser radiation, the processes mentioned above are present. Also, at low laser pulse energy/fluence regime, the temperature at the surface is slightly above the evaporation temperature thus the intensive material removal is possible *via* existence of a strong pressure in the absorbing region (Cheng & Xu, 2005; Nedialkov *et al.*, 2004). The ablated material, in this case, can include energetic nano-structures, which can be redeposited close to the crater. The fast transition from solid to vapor as well as fast cooling probably affect the material resolidification, including the appearance of a new crystallization form at the rim of the crater. Physics associated with nano-structures produced by laser ablation is very complex since they are described by the intermediate regime between quantum and classical physics. Their size depends, among other, on the laser repetition rate (Wang *et al.*, 2007).

Aside from morphological effects, femtosecond laser irradiation also causes local changes in the surface chemical composition of the material. EDX analysis of the Inconel 600 from different surface locations indicated on Figure 8 showed the occurrence of oxidation. Locations 1 and 2 of a non-irradiated region gave the results of surface elemental composition already mentioned in the introduction of this section. The oxygen content at the rim of the crater, locations 3 and 4, is increased, and the average enhancement as compared to a non-irradiated region was about 15%. Approximately the same increase of the oxygen content was registered at the periphery, i.e., in the zone of aggregates/nano-structures (spectra 5 and 6, Fig. 8). All of these results imply that the oxygen from air, during laser irradiation process, possesses high affinity to make oxide forms with elements from the target.

https://doi.org/10.1017/S0263034609990425 Published online by Cambridge University Press

4. CONCLUSION

A study of morphological changes of the nickel-based Inconel 600 super-alloy induced by a femtosecond Ti:sapphire laser, operating at high repetition rate of MHz range, is presented. Laser energy/fluence of maximum 20 nJ/15/mJ/cm^2, at the wavelength of 800 nm, was sufficient to induce surface modifications of the samples. The morphological modifications of the nickel-based super-alloy target can be summarized as follows: (1) intensive removal of surface material with crater like characteristics; (2) deposition of the material at near and farther periphery, including creation of nano-structures and their larger aggregates; (3) sporadic appearance of micro-cracking, especially at the rim area; and (4) appearance of plasma in front of the target. The ablation of Inconel 600 target surface is effective, resulting in holes with small diameter ($\leq$10 μm) and relatively high depth ($\leq$150 μm). The results for crater depths indicate a possibility of using femtosecond laser light in the precision drilling of μm size holes in thin foils of materials similar to Inconel.

Generally, we can conclude that with the average laser power of the order of watts, at high repetition rates (order of MHz) and lower pulse energies (order of nJ), the nickel-based super-alloy can be successfully modified, and the results are comparable to those obtained with low repetition rates (order of kHz) and higher pulse energies (order of mJ). Also, the femtosecond laser irradiation of the target gives smaller diameter and sharper damage, as compared to picosecond regime.

ACKNOWLEDGEMENTS

This research was sponsored by the Ministry of Science and Technological Development of the Republic of Serbia, Contract Nos. 142065 and 141003. Authors would like to thank Dr. M. Pavlovic (VINCA Institute of Nuclear Sciences, Belgrade) and Dr. G. Brankovic (Centre for Multidisciplinary Studies, Belgrade) for their help in conducting the target elemental analysis.

REFERENCES

Ancona, A., Röser, F., Rademaker, K., Limpert, J., Nolte, S. & Tünnermann, A. (2008). High speed laser drilling of metals using a high repetition rate, high average power ultrafast fibre CPA system. *Opt. Exp.* **16**, 8958–8968.

Bäuerle, D. (2003). Chapter 2 In Laser Processing And Chemistry. Berlin: Springer Verlag.

Bonse, J., Baudach, S., Krueger, J. & Kautek, W. (2000). Femtosecond laser micromachining of technical materials. *Proc. SPIE* **4065**, 161–172.

Bugayev, A.A., Gupta, M.C. & Payne, R. (2006). Laser processing of Inconel 600 and surface structure. *Opt. Laser Engin.* **44**, 102–111.

Busharov, N.P., Gusev, V.M., Guseva, M.I., Krasulin, Yu.L., Martynenko, Yu.V., Mirnov, S.V. & Rozina, I.A. (1977). Sputtering and blistering in the bombardment of Inconel, Sic + C alloy, and carbon-pyroceramic by H+ and He+ ions. *Atomic Energy* **42**, 554–559.

Bussoli, M., Batani, D., Desai, T., Canova, F., Milani, M., Trtica, M., Gakovic, B. & Krousky, E. (2007). Study of laser beam ablation with focused ion beam/scanning electron microscope devices. *Laser Part. Beams* **25**, 121–125.

Chaurasia, S., Munda, D.S., Ayyub, P., Kulkarni, N., Gupta, N.K. & Dhareshwar, L.J. (2008). Laser plasma interaction in copper nano-particle targets. *Laser Part. Beams* **26**, 473–478.

Chen, X., Lotshaw, W., Ortiz, A.L., Staver, P.R., Erikson, C.E., Mclaughlin, M.H. & Rockstroh, T.J. (1996). Laser drilling of advanced materials: effects of peak power, pulse format, and wavelength. *J. Laser Appl.* **8**, 233–239.

Cheng, C. & Xu, X. (2005). Mechanisms of decomposition of metal during femtosecond laser ablation. *Phys. Rev. B* **72**, 165415/1-15.

Di Bernardo, A., Courtous, C., Cros, B., Matthiewussent, G., Batani, D., Desai, T., Strati, F. & Lucchini, G. (2003). High-intensity ultrashort laser-induced ablation of stainless steel foil targets in the presence of ambient gas. *Laser Part. Beams* **21**, 59–64.

Eaton, S.M., Zhang, H., Herman, P.R., Yoshino, F., Shah, L., Bovatsek, J. & Arai, A.Y. (2005). Heat accumulation effects in femtosecond laser-written waveguides with variable repetition rate. *Opt. Exp.* **13**, 4708–4716.

Feng, Q., Picard, Y.N., Liu, H., Yalisove, S.M., Mourou, G. & Pollock, T.M. (2005). Femtosecond laser micromachining of a single-crystal superalloy. *Scr. Mater.* **53**, 511–516.

Gamaly, E.G., Madsen, N.R., Duering, M., Rode, A.V., Kolev, V.Z. & Luther-Davies, B. (2005). Ablation of metals with picosecond laser pulses: Evidence of long-lived nonequlibrium conditions at the surface. *Phys. Rev. B* **71**, 174405/1-12.

Hong, J.K., Park, J.H., Park, N.K., Eom, I.S., Kim, M.B. & Kang, C.Y. (2008). Microstructures and mechanical properties of Inconel 718 welds by CO_2 laser welding. *J. Mat. Process. Tech.* **201**, 515–520.

In, C.B., Kim, Y.I., Kim, W.W., Kim, J.S., Chun, S.S. & Lee, W.J. (1995). Pitting resistance and mechanism of TiN-coated Inconel 600 in 100°C NaCl solution. *J. Nucl. Mater.* **224**, 71–78.

Lam, Y.C., Tran, D.V. & Zheng, H.Y. (2007). A study of substrate temperature distribution during ultrashort laser ablation of bulk copper. *Laser Part. Beams* **25**, 155–159.

Liu, J.M. (1982). Simple technique for measurements of pulsed Gaussian-beam spot sizes. *Opt. Lett.* **7**, 196–198.

Ma, S., Mcdonald, J.P., Tryon, B., Yalisove, S.M. & Pollock, T.M. (2007). Femtosecond laser ablation regimes in a single-crystal superalloy. *Metall. Mater. Trans.* **38**, 2349–2357.

Mirdan, B.M., Jawad, H.A., Batani, D., Conte, V., Desai, T. & Jafer, R. (2009). Surface morphology modifications of human teeth induced by a picosecond Nd:YAG laser operating at 532 nm. *Laser Part. Beams* **27**, 103–108.

Nedialkov, N.N., Atanasov, P.A., Imamova, S.E., Ruf, A., Berger, P. & Dausinger, F. (2004). Dynamics of the ejected material in ultra-short laser ablation of metals. *Appl. Phys. A* **79**, 1121–1125.

Oh, B., Kim, D., Kim, J. & Lee, J.H. (2007). Femtosecond laser ablation of metals and crater formation by phase explosion in the high-fluence regime. *J. Phys: Confer. Ser.* **59**, 567–570.

Osellame, R., Chiodo, N., Maselli, V., Yin, A., Zavelani-Rossi, M., Cerullo, G., Laporta, P., Aiello, L., De Nicola, S.,

Ferraro, P., Finizio, A. & Pierattini, G. (2005). Optical properties of waveguides written by a 26 MHz stretched cavity Ti:sapphire femtosecond oscillator. *Opt. Exp.* **13**, 612–620.

Pantelis, D. & Psyllaki, P. (1996). Excimer laser micromachining of CMSX2 and TA6V alloys. *Mater. Manuf. Process.* **11**, 271–282.

Semaltianos, N.G., Perrie, W., French, P., Sharp, M., Dearden, G., Logothetidis, S., Semerok, A., Sallé, B., Wagner, J.F. & Petite, G. (2002). Femtosecond, picosecond, and nanosecond laser microablation: Laser plasma and crater investigation. *Laser Part. Beams* **20**, 67–72.

Semaltianos, N.G., Perrie, W., French, P., Sharp, M., Dearden, G., Logothetidis, S. & Watkins, K.G. (2009). Femtosecond laser ablation characteristics of nickel-based superalloy C263. *Appl. Phys A* **94**, 999–1009.

Tan, B., Panchatsharam, S. & Venkatakrishnan, K. (2009). High repetition rate femtosecond laser forming sub-10 μm diameter interconnection vias. *J. Phys. D: Appl. Phys.* **42**, 065102/1-9.

Trtica, M.S., Radak, B.B., Gakovic, B.M., Milovanovic, D.S., Batani, D. & Desai, T. (2009). Surface modifications of Ti6Al4V by a picosecond ND:YAG laser. *Laser Part. Beams* **27**, 85–90.

Wang, Y.L., Xu, W., Zhou, Y., Chu, L.Z. & Fu, G.S. (2007). Influence of pulse repetition rate on the average size of silicon nanoparticles deposited by laser ablation. *Laser Part. Beams* **25**, 9–13.

Zysk, K.T. (1990). Pulsed CO_2 laser welding of Inconel 718. Proc. AIAA, SAE, ASME, ASEE 26th Joint Propulsion Conference, 10.